

An isotopic effect in self-assembly of amphiphilic block copolymers: the role of hydrogen bonds†

Rina Shvartzman-Cohen,^a Chun-lai Ren,^b Igal Szleifer^{*c} and Rachel Yerushalmi-Rozen^{*ad}

Received 1st July 2009, Accepted 18th September 2009

First published as an Advance Article on the web 26th October 2009

DOI: 10.1039/b913005e

An isotopic effect was observed in solutions of self-assembling (SA) amphiphilic block copolymers: it was found that the micellization enthalpy, temperature and the size of the formed micelles are affected by replacing H₂O by D₂O. The SA of solvated block-copolymers (poly(ethylene oxide)–poly(propylene oxide)–poly(ethylene oxide)) in H₂O, D₂O and their mixtures was investigated as a function of temperature. High sensitivity differential scanning calorimetry revealed that the micellization temperature is reduced, and the enthalpic penalty of the transition and size of the formed micelles increase when H₂O is exchanged by D₂O. Molecular theory calculations suggest that the difference in the hydrogen bond strength of the solvent, H₂O or D₂O, is the origin of the different structural and conformational properties of the solvated block copolymers. The differences in the solvent properties were predicted to modify the solubility and consequently the SA of the polymers in the two solvents, as experimentally measured. The study provides an insight into the role of hydrogen bonding in systems of amphiphilic block copolymers, and suggests that in SA polymers small differences in hydrogen-bonding strength of the solvent may result in observable macroscopic effects.

1. Introduction

The spontaneous self assembly of non-ionic block-copolymers, such as (poly(ethylene oxide)–poly(propylene oxide)–poly(ethylene oxide)), PEO_y–PPO_x–PEO_y (Ploxamers (ICI) or Pluronics (BASF)) in water into micellar structures, is utilized in a wide range of applications including detergency, dispersion stabilization,¹ foaming, emulsification,² formulation of cosmetics^{3,4} and inks,⁵ drug solubilization and controlled release.^{6–8}

At room temperature and low polymer concentrations, water acts as selective solvent for the Pluronic block copolymers: It is a good solvent for PEO,⁹ and a moderate solvent for PPO. Water becomes a less good solvent for both PPO and PEO when the concentration or temperature are increased¹⁰ and drives micellization that is followed by phase separation.¹¹

The solubility of Pluronic in water is attributed to hydrogen bonding between the hydrogen atoms of water and the ether oxygen of the polymer backbone.¹¹ The strong dependence of the solvent quality on temperature is related to the formation and rupture of the polymer coil hydration shell and of the hydrogen-bond (HB) network in the bulk solvent. The latter is affected by the temperature, and at a given temperature micelles form at the critical micellar concentration (cmc), and at a given (low)

concentration micellization occurs at the critical micellization temperature (cmt). The micellar structures consist of a PPO core and a corona of solvated PEO. It is well known that the dehydration of water from the PPO blocks drives the onset of micellization, while the variation of the size and geometry of the micelles with temperature depends mostly on the gradual dehydration of PEO blocks.^{11,12} A transition from spherical to elongated (rod-like) micelles is observed in micelles formed by copolymers of intermediate PEO size.^{13,14} Thus, temperature is often used as a control parameter for tuning the structure and size of Pluronic micelles.

The micellization process of PEO–PPO–PEO block copolymers as well as other amphiphilic polymers has been investigated thoroughly, often by methods that rely on isotopic substitution of H₂O by D₂O. In particular, X-ray and neutron-scattering have utilized D₂O so as to achieve favorable contrast in scattering length density.^{14,15} Electron spin resonance (ESR) was used to probe the molecular details in deuterated solutions.¹⁶

Thus, an important portion of our current knowledge of this system, as well as other amphiphilic systems, was derived under the implicit assumption that the bulk physical chemistry is unchanged by an isotopic exchange of H₂O with D₂O. Yet, as has been demonstrated before,^{17–19} H/D substitution is not a true isomorphic replacement, and isotopic effects are found to play a key role in phenomena which are sensitive to the nuclear structure or bond polarizability.

Here we present high-sensitivity differential scanning calorimetry (HSDSC) measurements and molecular theory calculations of the self-assembly (SA) of Pluronic in H₂O, D₂O and mixtures of these solvents, as a function of temperature and polymer concentration. We show that SA of Pluronic block-copolymers is sensitive to the replacement of H₂O by D₂O, and isotopic exchange results in a distinguishable micellization behavior.

^aDepartment of Chemical Engineering, Ben-Gurion University of the Negev, 84105 Beer-Sheva, Israel

^bNational Laboratory of Solid State Microstructures, Nanjing University, Nanjing, 210093, China

^cDepartment of Biomedical Engineering, Northwestern University, 2145 Sheridan Rd., Evanston, IL, 60208, USA

^dThe Ilze Katz Institute for Nanoscale Science & Technology, Ben-Gurion University of the Negev, 84105 Beer-Sheva, Israel

† Electronic supplementary information (ESI) available: Numerical method. See DOI: 10.1039/b913005e

The molecular theory applied here has been originally developed to study the packing and SA of short surfactant aggregates, and was later generalized to treat polymer layers.^{20–24} More recently, the theory has been extended to explicitly include HB between the polymers and the solvent.²⁵ We show that by taking into account the difference in HB strength in water as compared to its deuterated counterpart, one is able to explain the experimental observations of Pluronic SA in the two solvents as well as in their mixtures. Furthermore, we show the diameter of the formed micelles depend on the solvent. For mixed solvents we find that solvent partitioning within the micellar aggregates is not random. Our ability to calculate the effect of the HB strength on the solubility and self-assembly of the polymers in the two solvents provides an insight into the role of HB in the SA of amphiphilic block copolymers.

2. Materials and methods

Materials

Pluronic triblock copolymers were received as a gift from BASF AG Germany and used as received. The polymers are listed in Table 1.

Techniques and methods

High-sensitivity differential scanning calorimetry (HSDSC). Microcal VP-DSC for HSDSC, at cell volume of 0.5 ml was used. The reported measurements were carried out at a scan rate of 1 K min⁻¹, by heating from 280 K to 360 K. The HSDSC instrument measures the power required to keep the temperature of the sample and reference cell equal, while raising the temperature of the system at a constant rate. The output of the instrument is $(dq/dt)_p$ vs. t , where q is the heat and t is time. The output is converted to the excess heat capacity (C_p) vs. temperature by multiplying the x axis by the scan rate. Exploratory measurements carried at different scan rates suggested that the calorimetric data was not affected by the scan rate. Heating and cooling sequences did not show hysteresis. To estimate the uncertainties in the measurement, multiple heating and cooling scans were carried out, suggesting an uncertainty of $\pm 5\%$ in the calorimetric enthalpy and 0.1 °C in the cmt.

DSC allows the evaluation of thermodynamic properties as heat capacity and transition temperatures over the scanned temperature range, thus providing information about the enthalpy of the micellization process and the micellization onset temperature. Micellization of Pluronic-type block copolymers is characterized by the appearance of an asymmetric endothermic peak. It is well accepted that the peak results from the

dehydration of the PPO groups and that the enthalpy of the transition is proportional to size of the PPO moiety of the polymer.^{10,11}

Theoretical approach

To interpret the experimental observations, we apply a molecular theory that has been shown to provide very good quantitative agreement with experimental observations for the structure and thermodynamic properties of chain molecules at surfaces, interfaces and the self-assembly of short-chain molecules.^{20–24} In recent work,²⁵ we have studied the properties of end-tethered PEO layers with explicit inclusion of HB. In the present work we generalize the theory to study SA of amphiphilic polymers and explicitly include HB. In particular we investigate the effect of the difference in HB strength (between hydrogen and deuterium) on the SA of polymeric micelles. We present a simplified version of the theory, with the aim of stressing the novel features due to the consideration of hydrogen bonds. For more details the reader is referred to ref. 24–26.

We consider only the case of dilute solutions where the micellization is well described by the mass action model.²⁷ Namely, we assume an ideal dilute solution of micelles, and the condition of thermodynamic equilibrium is that the chemical potential of the polymers is identical whether they are in micelles or isolated in a homogeneous solution. Thus, the micellar size distribution within this model is given by $X_N = N[X_1 \exp(-\beta\Delta F_N)]^N$, where $\Delta F_N = F_N - F_1$ is the difference in free energy between a polymer isolated in solution and within an aggregate of size N . The size distribution has to fulfil the constraint that the total solution concentration of polymers is given by $c = \sum_i iX_i$. We define the cmc as the concentration

where the number of molecules in the form of single chains in solution is equal to those in micellar aggregates. Namely, $X_1 = \sum_{i=2} X_i$. Once cmc is presented as a function of temperature, the cmt may be deduced by noting the temperature at which micellization occurs for a given concentration (see Fig. 6 and discussion thereafter).

Thus, in the limit of ideal solution of micelles all that is needed to determine micellization and the distribution of sizes are the differences in the free energy of formation of the different size aggregates. The latter is obtained from the molecular theory.

For simplicity, we consider only spherical aggregates, the extension to other geometries is straightforward but beyond the scope of the present work. We use spherical coordinates where r denotes the radial distance from the center of the micelle. The free energy of a micelle composed of N polymers is given by eqn (1), where $\beta = 1/k_B T$ is the inverse absolute temperature.

The first term is the conformational entropy of the chains, with $P(\alpha)$ being the probability of finding a polymer chain in conformation α , and the sum running over all the conformations of the chains. The second term is the distance-dependent translational (mixing) entropy of the water molecules, with $\rho_w(r)$ being the density of water at position r . The third term represents the van der Waals water–PEO, water–PPO and PEO–PPO

Table 1 List of triblock copolymers

Polymer	MW	No. of EO units	No. of PO units	PEO (wt%)	Product no.
L64	2900	26	30	40	576320
F88	11400	200	40	80	560840
P103	4950	32	56	30	586460
F108	14600	260	60	80	583062
P123	5750	40	70	30	587440
F127	12600	212	70	70	583106

$$\begin{aligned}
\beta F_N = N \sum_{\alpha} P(\alpha) \ln P(\alpha) + \int dr 4\pi r^2 \rho_w(r) [\ln \rho_w(r) v_w - 1 - \beta \mu_w] + \\
\int dr 4\pi r^2 \left[\frac{\chi_{eo-w}}{v_w} \langle \phi_{eo}(r) \rangle \phi_w(r) + \frac{\chi_{po-w}}{v_w} \langle \phi_{po}(r) \rangle \phi_w(r) + \frac{\chi_{eo-po}}{v_w} \langle \phi_{eo}(r) \rangle \langle \phi_{po}(r) \rangle \right] + \\
\int dr 4\pi r^2 \beta \pi(r) [\langle \phi_{eo}(r) \rangle + \langle \phi_{po}(r) \rangle + \phi_w(r)] + \beta F_{hb}
\end{aligned} \tag{1}$$

interactions respectively, where $\langle \phi_i(r) \rangle$ represents the average volume fraction of segments of type i ('eo' and 'po') at distance r from the center of the micelle, and it is given by

$$\langle \phi_i(r) \rangle = \frac{1}{V(r)} \sum_{\alpha} P(\alpha) v_i(r; \alpha) \tag{2}$$

where $V(r)$ is the volume in the layer between r and $r + dr$ and $v_i(r; \alpha)$ is the volume of segments of type i that a polymer in conformation α occupies between r and $r + dr$. $\phi_w(r) = \rho_w(r) v_w$ is the volume fraction of water and χ_j ($j = eo-w, po-w$ and $eo-po$) are the strength of the eo-water, po-water and eo-po interactions respectively. The fourth term accounts for the excluded-volume repulsive interactions between all the molecules, where $\pi(r)$ represents the average repulsive interaction field and is related to the distance-dependent osmotic pressure. The last term is the free energy of the hydrogen bonds and for the case of H₂O and Pluronic is given by eqn (3).

The derivation of the different terms for inhomogeneous environments are discussed in ref. 25 and are inspired by the work of Dormidontova.^{28,29} Here we point out their origins considering the possibility of water-water, water-EO and water-PO hydrogen bonds and taking into account that water can be a hydrogen bond acceptor and donor while the EO and PO segments can only be hydrogen bond acceptors. $\rho_i(r)$

is the number density of segments of type i and $x_i(r)$ denotes the fraction of segments of type $i = w, eo$ or po , that participate in hydrogen bond (HB) at position r , and ΔF_i is the intrinsic free energy of a single hydrogen bond of type i . The competition between the different types of HB results from the interplay between the entropy, which tends to randomize the different types of bonds and the intrinsic free energy for each HB pair, which favors water-water interactions over water-polymer interactions (see discussion in ref. 25 and 26).

To find the density profile for all the molecular species, the probability of each of the polymer chain conformations and the fraction of the different HB with their spatial variation we minimize the total free energy. This yields for the probability of chain conformations eqn (4), where $V(\alpha, r)$ is a geometric factor to account for the available volume at distance r from the center of the micelle, q is the normalization constant and there are three different contributions in the Boltzmann factor arising from the repulsive interactions, the HB and the van der Waals interactions respectively.

The volume fraction of water from the minimization is given by eqn (5), while the fraction of HB for the water, EO and PO segments as a function of the radial distance are given by the three equations (6).

$$\begin{aligned}
\beta F_{hb} = \int dr 4\pi r^2 2\rho_{eo}(r) [x_{eo}(r) \ln x_{eo}(r) + (1 - x_{eo}(r)) \ln(1 - x_{eo}(r)) - x_{eo}(r) \beta \Delta F_{eo}] + \\
\int dr 4\pi r^2 2\rho_{po}(r) [x_{po}(r) \ln x_{po}(r) + (1 - x_{po}(r)) \ln(1 - x_{po}(r)) - x_{po}(r) \beta \Delta F_{po}] + \\
\int dr 4\pi r^2 2\rho_w(r) [x_w(r) \ln x_w(r) + (1 - x_w(r)) \ln(1 - x_w(r)) - x_w(r) \beta \Delta F_w] + \\
\int dr 4\pi r^2 2\rho_w(r) \left[1 - x_w(r) - \frac{x_{eo}(r) \rho_{eo}(r)}{\rho_w(r)} - \frac{x_{po}(r) \rho_{po}(r)}{\rho_w(r)} \right] \ln \left[1 - x_w(r) - \frac{x_{eo}(r) \rho_{eo}(r)}{\rho_w(r)} - \frac{x_{po}(r) \rho_{po}(r)}{\rho_w(r)} \right] - \\
\int dr 4\pi r^2 2\rho_w(r) \left[x_w(r) + \frac{x_{eo}(r) \rho_{eo}(r)}{\rho_w(r)} + \frac{x_{po}(r) \rho_{po}(r)}{\rho_w(r)} \right] \ln \frac{2\rho_w(r) v_w}{e}
\end{aligned} \tag{3}$$

$$\begin{aligned}
P(\alpha) = \frac{V(\alpha, r)}{q} \exp \left\{ - \int dr \beta \pi(r) [v_{eo}(\alpha, r) + v_{po}(\alpha, r)] - 2 \int dr \{ n_{eo}(\alpha, r) \ln [1 - x_{eo}(r)] + n_{po}(\alpha, r) \ln [1 - x_{po}(r)] \} \right\} \\
\exp \left\{ - \int dr \left[\frac{\chi_{eo-w}}{v_w} v_{eo}(\alpha, r) \phi_w(r) + \frac{\chi_{po-w}}{v_w} v_{po}(\alpha, r) \phi_w(r) + \frac{\chi_{eo-po}}{v_w} v_{eo}(\alpha, r) \langle \phi_{po}(r) \rangle + \frac{\chi_{eo-po}}{v_w} v_{po}(\alpha, r) \langle \phi_{eo}(r) \rangle \right] \right\}
\end{aligned} \tag{4}$$

$$\phi_w(r) = \rho_w(r)v_w = \exp[\beta\mu_w - \beta\pi(r)v_w - \chi_{eo-w}\langle\phi_{eo}(r)\rangle - \chi_{po-w}\langle\phi_{po}(r)\rangle - 2(\ln x_w(r) - \ln 2\rho_w(r)v_w - \beta\Delta F_w)] \quad (5)$$

$$\begin{aligned} \ln x_w(r) - \ln(1 - x_w(r)) - \beta\Delta F_w &= \ln\left[1 - x_w(r) - \frac{x_{eo}(r)\rho_{eo}(r)}{\rho_w(r)} - \frac{x_{po}(r)\rho_{po}(r)}{\rho_w(r)}\right] + \ln 2\rho_w(r)v_w \\ \ln x_{eo}(r) - \ln(1 - x_{eo}(r)) - \beta\Delta F_{eo} &= \ln\left[1 - x_w(r) - \frac{x_{eo}(r)\rho_{eo}(r)}{\rho_w(r)} - \frac{x_{po}(r)\rho_{po}(r)}{\rho_w(r)}\right] + \ln 2\rho_w(r)v_w \\ \ln x_{po}(r) - \ln(1 - x_{po}(r)) - \beta\Delta F_{po} &= \ln\left[1 - x_w(r) - \frac{x_{eo}(r)\rho_{eo}(r)}{\rho_w(r)} - \frac{x_{po}(r)\rho_{po}(r)}{\rho_w(r)}\right] + \ln 2\rho_w(r)v_w \end{aligned} \quad (6)$$

The density profiles, probability distribution and fraction of HB are determined by placing eqns (2), (4), (5) and (6) into the packing constraints

$$\langle\phi_{eo}(r)\rangle + \langle\phi_{po}(r)\rangle + \phi_w(r) = 1 \quad \text{for all } r$$

which leads to a set of coupled non-linear equations for the osmotic pressures that are solved self-consistently. Detailed information describing how the equations are solved, how the chains are generated and the origin of the parameters set used can be found in the ESI†. The expressions derived in this section correspond to a pure solvent, *i.e.* water or D₂O. For the cases of mixtures of solvents the equations have to be generalized, as is shown in the ESI. The ESI also includes the choice of parameters used in all the calculations. However, a proper quantitative evaluation is difficult to obtain, as systematic solubility studies of PPO and PEO in water at different conditions, at the relevant temperature range, are not available. It should be mentioned the physical insights are not affected as we use the same value of χ_{po-w} for H₂O and D₂O. Aiming to investigate the role of the *solvent* hydrogen bonds (the reference state), we fix the free energies of the polymer–solvent hydrogen bond to the value of the PEO–water case. The strength of the D₂O–D₂O hydrogen bond is taken to be 5% stronger than that of the hydrogenated solvent. This strategy enables us to overcome the difficulties imposed by the lack of experimental data, and yet investigate the qualitative behavior and probe the role of the *solvent* hydrogen bonds on the observed behavior of the polymers in water *vs.* D₂O.

3. Results and discussion

Thermal characterization of Pluronic SA from solutions of H₂O and D₂O

HSDSC was used to examine the temperature- induced SA of different Pluronic block copolymers in H₂O, D₂O, and D₂O–H₂O mixtures. As can be seen in the thermograms (Fig. 1), micellization of Pluronic block copolymers is characterized by the appearance of an asymmetric endothermic peak. It is well accepted that the peak results from the dehydration of the PPO groups, and that the entropic gain by water molecules due to dehydration of the PPO blocks drives the process.^{10–12,31,32}

Similar behavior is observed for the different block copolymers: when H₂O is replaced by D₂O the enthalpy of the

micellization process increases significantly and the onset of micellization (cmt) is shifted to lower temperatures. The values of the enthalpy change (ΔH_{cal}) related to the micellization process as calculated from integration of C_p *vs.* T and the cmt of 5 different polymers are summarized in Table 2.

The difference between the measured values of H₂O and D₂O solutions are summarized in Table 3.

The data presented in Table 3 suggest that for 1 wt% polymer solutions the enthalpy of micellization is typically higher by 10–15% in D₂O solutions than in H₂O, while a significantly higher difference (about 30%) is observed in solutions of F88. In all the measured solutions cmt values are shifted to lower temperatures in D₂O solutions compared to H₂O. Here again the shift is significantly higher for F88, which exhibits the highest difference in the transition enthalpies between D₂O and H₂O. The initial slope is steeper by about 20% than in H₂O solutions, indicating the formation of larger aggregates, and suggesting “higher cooperativity”.^{30–33}

D₂O volume fractions. The effect of D₂O volume fraction on the cmt of F88, P123 and F108 (1 wt%) was examined. In Fig. 2 we present the behavior of P123.

We observe that cmt values decrease and the enthalpy of the transition increases monotonically as the volume fraction of D₂O increase, as presented in Table 4.

The data presented in Fig. 3 indicate that the dependence of cmt on the volume fraction of D₂O is not linear, but rather saturates with the D₂O volume fraction. We relate to this point in the theoretical section.

An interesting observation is revealed by thermograms of P123. As can be seen in Fig. 4a, P123 (1 wt%) solutions in pure water exhibit (in the temperature range 10–70 °C) two thermal transitions: micellization and a transition from spherical to elongated micelles (marked by the smaller peak).¹⁰ Above a D₂O volume fraction of 0.5 (Fig. 4b, inset) a new peak is visible. The peak is located at an intermediate temperature located between the micellization and spherical-to-elongated micelle transitions. The peak is of a much lower enthalpy than the peak marking the micellization, but is rather narrow. The shape of the peak may suggest the appearance of a new morphological transition, yet DSC does not provide structural information. Such information may be obtained by scattering techniques.

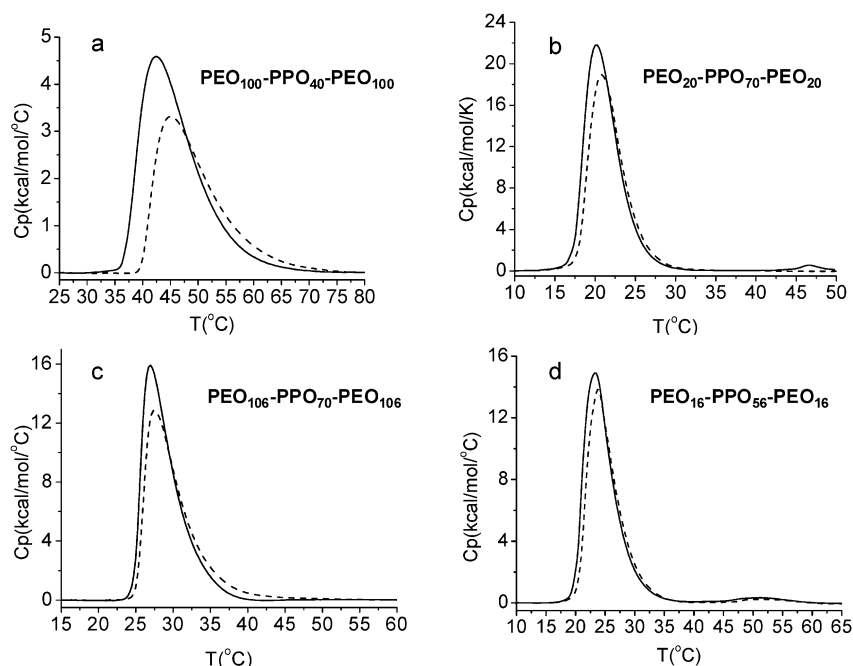


Fig. 1 DSC thermograms of 1 wt% solutions in water (dashed line) and D₂O (solid line): (a) F88, (b) P123, (c) F127, and (d) P103.

Table 2 ΔH_{cal} and cmt of Pluronic micellization in H₂O and D₂O in 1 wt% solutions of Pluronic block copolymers

Polymer	H ₂ O		D ₂ O	
	Area/kcal mol ⁻¹ °C ⁻¹	cmt/°C	Area/kcal mol ⁻¹ °C ⁻¹	cmt/°C
L64	42.0	32.1	48.4	31.3
P103	84.6	22.6	95.5	21.7
P123	97.9	18.9	111.7	18.3
F88	41.6	41.3	55.1	38.7
F127	73.3	27.2	86.4	26.8

Table 3 Differences in the calorimetric parameters of Pluronic micellization in H₂O and D₂O as measured by DSC experiments

Polymer	Composition	$\Delta H_{\text{D}_2\text{O}}/\Delta H_{\text{H}_2\text{O}}$ (%)	Δcmt	Slope ratio ^a
L64	PEO ₂₆ , PPO ₃₀	1.15	0.8	1.1
P103	PEO ₃₂ , PPO ₅₆	1.1	0.9	1.2
P123	PEO ₄₀ , PPO ₇₀	1.13	0.6	1.2
F88	PEO ₂₀₀ , PPO ₄₀	1.32	2.6	1.2
F127	PEO ₂₁₂ , PPO ₇₀	1.18	0.4	1.3

^a Slope ratio is defined as the ratio of the maximal slope at the leading edge of the peak in D₂O as compared to H₂O.

Molecular theory. In the following we present a detailed theoretical description of Pluronic SA in D₂O vs. H₂O. Before presenting the results it is important to emphasize that the aim of the theoretical calculations is not to provide a quantitative description of the experimental observations, but rather to gain a fundamental molecular understanding of how differences in the HB strength between H₂O and D₂O lead to observed differences in the aggregation behavior of the polymers. A quantitative comparison is not attempted as values of the interaction

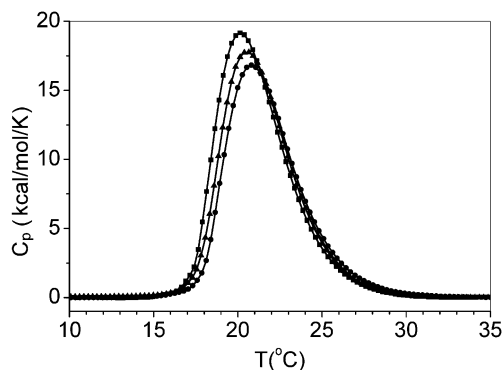


Fig. 2 DSC thermograms of 1 wt% P123 in pure D₂O (■) H₂O (●) and an equi-volume mixture of 0.5 D₂O (▲).

Table 4 ΔH_{cal} and cmt of different D₂O volume fractions for P123 and F88 (1 wt%) solutions

D ₂ O volume fraction	1 wt% P123		1 wt% F88	
	Area/kcal mol ⁻¹	cmt/°C	Area/kcal mol ⁻¹	cmt/°C
1	111.4	18.3	55.4	38.7
0.9	105.5	18.4	50.7	39.7
0.5	98.8	18.8	42.4	40.7
0.1	93.4	18.9	39.5	41.2
0	98.2	18.9	41.9	41.3

parameters that are required as input are not well known, as is the case for example for the strength of the HB between PPO and water. Thus, rather than fitting the parameters, we show that 5% differences in HB strength between H₂O and D₂O (keeping all the other interactions identical), qualitatively explain the experimental observations.

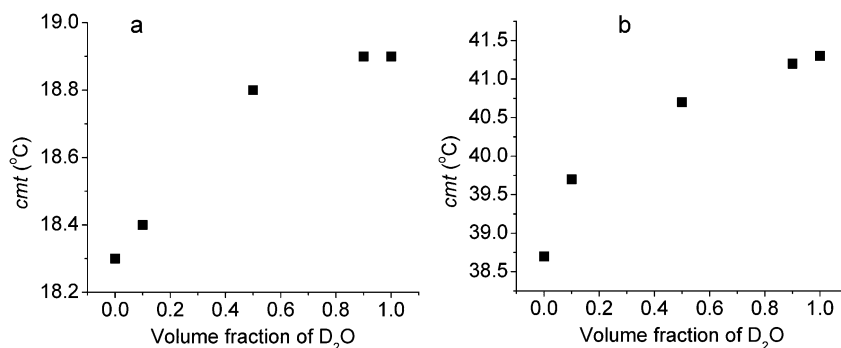


Fig. 3 cmc as a function of D₂O volume fraction for (a) 1 wt% P123 and (b) 1 wt% F88.

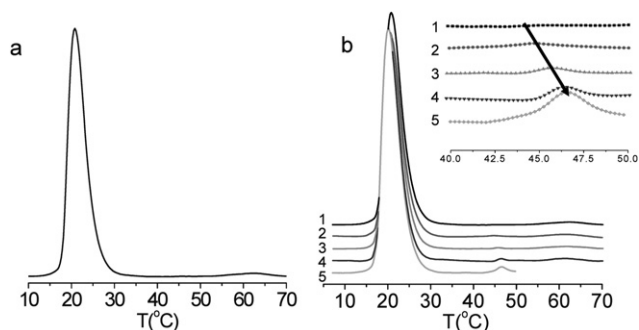


Fig. 4 DSC thermograms of 1 wt% P123 (a) in pure H₂O and (b) in solutions of 5 different D₂O volume fractions. Inset: (1) pure H₂O, (2) 0.1 D₂O, (3) 0.5 D₂O, (4) 0.9 D₂O, (5) pure D₂O.

The SA in the dilute regime is completely determined by the free energy of micellization. Namely, the free energy per molecule as a function of the number of molecules in the aggregate. This is shown in Fig. 5 for P103 in three different solvents, pure H₂O, pure D₂O and an equimolar mixture. The free energy shown corresponds to the difference between that of a polymer chain of aggregate N and that of an isolated polymer molecule in the solvent. Before analyzing the differences between the three cases

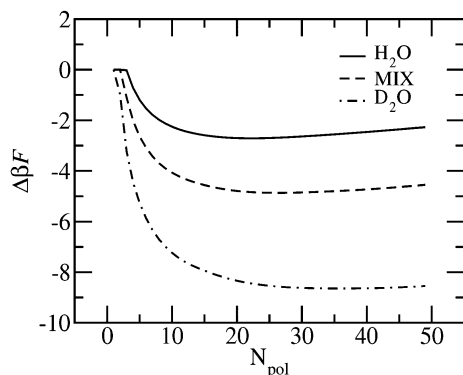


Fig. 5 The free energy difference between a polymer in an aggregate of size N_{pol} and an isolated polymer in solution for model Pluronic P103 as a function of the size of the aggregate for three different solvents, as marked in the figure, at $T = 25$ °C. Note that for H₂O and the mixed solvent the curve is flat for small N_{pol} , since the polymer prefers the isolated state to small aggregates.

it is important to understand that the micellization, *i.e.* the cmc, is determined by the free energy difference between a single chain and the minimum of the curve that represents the free energy gained by a molecule in an aggregate. This difference is typically a few times the thermal energy ($k_{\text{B}}T$) per molecule, and therefore micelles are highly favored. The size distribution however, as is shown below, depends on the free energy differences around the minimum and therefore the difference between sizes is determined by small fractions of $k_{\text{B}}T$ per molecule (see ref. 22 for a thorough discussion of this effect).

The free energies presented in Fig. 5 show the dramatic effect of the solvent on the free energy of aggregation. Micellization is a much more favored process in D₂O as compared to H₂O, on the order of $6 k_{\text{B}}T$ per Pluronic molecule at the presented temperature. This effect is due exclusively to the differences in the strength of the hydrogen bonding between water and its deuterated counterpart. Solvation of polymer molecules forces some of the solvent molecules to form HB with the polymer chain. Each of these bonds results in a free energy penalty for the solvent molecules, and as the number of solvent–polymer HB increases, so does the free energy cost. As we show below, the number of HB formed between Pluronic aggregates and D₂O is smaller than with H₂O molecules, and thus the micellization results in a lower loss of HB for D₂O, resulting in a much larger free energy of micellization, *i.e.* a larger difference between the free energy per molecule of a single chain as compared to the free energy per molecule in the aggregate.

Interestingly, the same effect explains why the minimal free energy corresponds to larger aggregates for D₂O as compared to H₂O and the solvent mixtures. Furthermore, we find (Fig. 5) that the free energy as a function of the micellar size in the equimolar mixture of the solvents is not the average of the values in the pure solvents. This implies that the micellization process involves non-ideal mixing, or a non random partitioning of the solvent in the micelles as compared to the bulk. This point is further discussed below. Note that for H₂O and the mixed solvent the curve flattens (Fig. 5) for the smallest aggregation numbers (small N_{pol}), suggesting that the polymer prefers to be dissolved as individual molecules rather than form small aggregates. This is another demonstration of the difference in quality of solvent for the three cases.

From the dependence of the free energy on the aggregate size for each temperature, we can obtain the cmc as a function of temperature. We define the cmc as the concentration where the

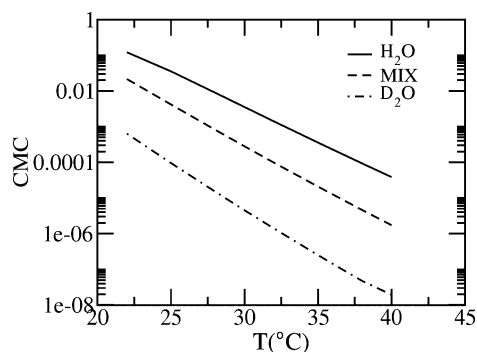


Fig. 6 Predicted cmc for P103 as a function of temperature in H₂O, in an equimolar mixture, and in D₂O. The cmt is the temperature of micellization for a fixed polymer concentration.

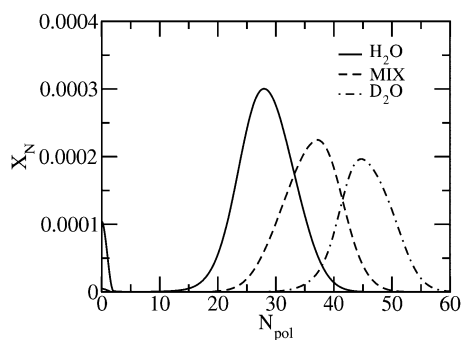


Fig. 7 Distribution of the aggregation number in H₂O (solid line), D₂O (dashed line) and an equimolar mixture (dot-dashed line). The calculations correspond to a total polymer volume fraction of 0.1 and temperature $T = 40$ °C for Pluronic P103.

number of polymer chains that are dissolved as individual chains equals the number of aggregated polymers. Fig. 6 shows the cmc as a function of temperature for the two pure solvents and their equimolar mixture. In the three cases as the temperature increases the cmc decreases showing the reduction of solubility of both PEO and PPO with increasing temperature. The variation of the critical micellar concentration with temperature is close to exponential but not exactly. This is due to the non-trivial dependence of the free energy of micellization on temperature. Interestingly, the three curves are not exactly parallel to each other, demonstrating that HB effects are not simply additive as has been discussed for the different free energy curves of Fig. 5 and observed experimentally (Fig. 3).

The predicted cmc values are two orders of magnitude lower in D₂O than in H₂O. We see that the predicted trends of the aggregation are similar to those measured experimentally (Tables 2–4). This again is a direct manifestation of the fact that the D₂O–D₂O HB is stronger than that of water. Note that a difference of 5% in the strength of the HB results in a (predicted) change of 5 to 10 °C in the cmt.

Fig. 7 presents the distribution of aggregates size in pure H₂O, D₂O and a symmetric mixture. We find that for a specific concentration above cmc (at constant temperature) both the aggregation number (comprising a single micelle) and the volume fraction of micelles are higher in D₂O than in H₂O. This

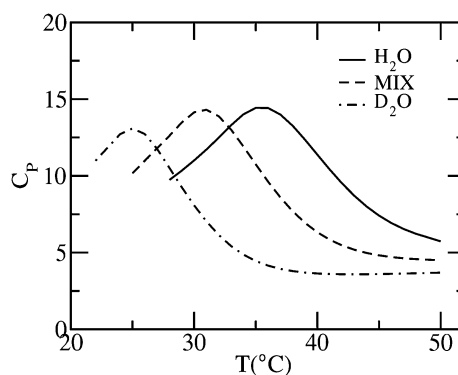


Fig. 8 Calculated constant-pressure heat capacities as a function of temperature for Pluronic L64 for aggregates of aggregation number $N_{\text{pol}} = 20$.

observation is in good agreement with the steeper slope of D₂O solutions, measured in the DSC experiments (Figs. 1 and 2, Table 3). Again this phenomenon can be attributed to the gain in the number of hydrogen bonds among solvent molecules that results from aggregation of a larger number of molecules into micelles.

Fig. 8 displays the constant-pressure heat capacities calculated from the theory. The heat capacity is obtained from $C_p = T(\delta S / \delta T)_p$ where the entropy is obtained by differentiation of the free energy expression derived above with respect to the temperature. These results can be compared with the C_p values measured in the DSC experiments. Clearly, the predicted curves show the same trends observed experimentally: The peak in the C_p shifts to lower temperatures for D₂O as compared to the equimolar mixture and pure water. At this point it is important to emphasize that the predicted differences between the solvents in the transition temperatures are much larger than the measured experimentally, as discussed below.

Fig. 9 displays the density profiles of the PPO (left panel) and PEO (right panel) moieties as a function of the distance from the center of the micelle for the three different solvents. The temperature and the number of the polymer molecules is fixed. The profiles clearly display the important role of HB in the structure of the micelles. Fig. 9 shows that micelles in D₂O are very compact, with minimal penetration of the solvent into the hydrophobic (PPO) core. Furthermore, as can be seen at distances around $r \approx 3$ nm the interface between the hydrophobic core and the solvent is much sharper when D₂O is the solvent. This is another manifestation of the fact that the relative quality of the solvent is determined by the strength of the solvent–solvent HB. As D₂O is the lower-quality solvent, a more compact structure emerges. Interestingly, the PEO block is very similar in the equimolar mixture of solvents and the H₂O case.

To complete the analysis of the structure of the micelles, Fig. 10 shows all the density profiles for a micelle in an equimolar mixture of solvents. The shapes of the PPO and PEO blocks are similar to those presented in Fig. 9. The interesting part is that the solvent does not partition randomly when in contact with the polymer. The profiles clearly show that water preferably resides in the vicinity of the polymer. In other words, the free energy cost of polymer solvation by water is lower than polymer solvation by D₂O. Again this is due to the fact that in this way the system

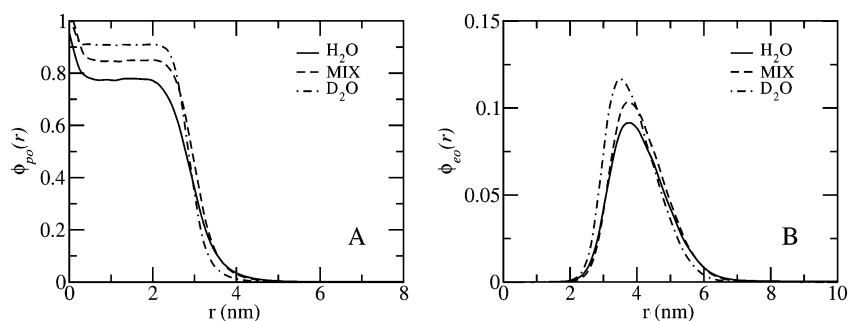


Fig. 9 Calculated density profiles of PPO (left panel) and PEO (right panel) as a function of the distance from the micelle center for H₂O (solid line), D₂O (dashed line) and an equimolar mixture (dot-dashed line). The calculations correspond to Pluronic P103 with aggregation number $N_{\text{pol}} = 20$ and $T = 25$ °C.

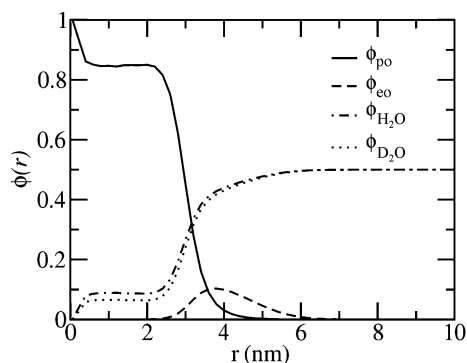


Fig. 10 Calculated density profiles of a micelle in an equimolar mixture of solvents. The calculations correspond to Pluronic P103 with aggregation number $N_{\text{pol}} = 20$ and $T = 25$ °C.

gains a larger number of the more favorable D₂O–D₂O HBs. This is clearly observed in Fig. 11 where the fraction of HBs as a function of the distance from the center of the micelles is shown. The fraction of propylene oxide deuterium HBs is lower than that of the polymer and hydrogen (Fig. 11B) in the hydrophobic core of the micelle, while the water–water HBs are larger than the D₂O–D₂O HBs. The fraction of HBs between the two types of solvent, though, is inverted in the bulk solution, where there is a larger fraction of D–D HBs than H–H HBs.

The HB behavior observed in Fig. 11 results from the best compromise between the preference of D₂O to form hydrogen bonds with itself and the entropy of mixing. By segregating the poorer solvent into the solution the system finds its optimal state.

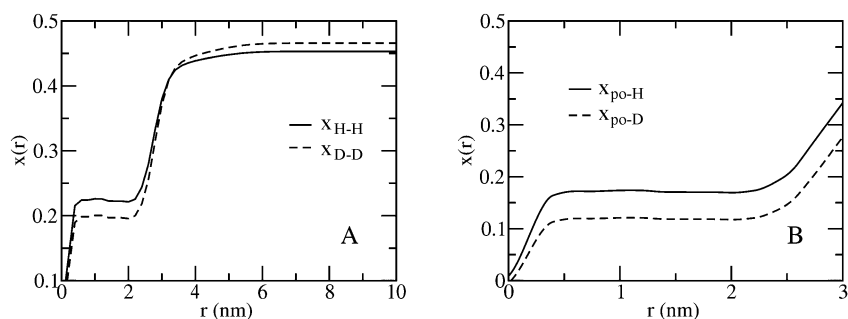


Fig. 11 The fraction of solvent–solvent (A) and polymer–solvent (B) hydrogen bonds as a function of the distance from the center of the micelle. The conditions are the same as in Fig. 10.

5. Conclusions

Experimental observations reveal that the SA of amphiphilic block copolymers is significantly affected by an isotopic exchange of the solvent. Replacement of H₂O by D₂O affects the micellization temperature, enthalpy, and size of the formed micelles. Molecular theory calculations indicate that the difference in HB between H₂O–H₂O and D₂O–D₂O are the origin of the observed phenomena. The calculations demonstrate that small differences in the strength of HB are enough to induce a large change in the free energy of solvation of the polymers, and consequentially (i) lower the cmt of the triblock copolymers in D₂O, (ii) induce a more compact structure and a larger aggregation number and (iii) shift the size distribution to higher values. A qualitative description would suggest that as the solvent–solvent hydrogen bonding becomes stronger (while the strength of the polymer solvent HB is retained), the solvent becomes poorer for the chain molecules. It is important to emphasize, however, that the solvent quality here is not determined by van der Waals interactions but rather by the competitive nature of the HBs between two solvent molecules compared to a solvent and a polymer.

The study provides an insight into the role of hydrogen bonding in systems of amphiphilic block copolymers, and suggests that in SA polymers small differences in hydrogen bonding strength of the solvent may result in observable macroscopic effects. These observations suggest that the common assumption that isotopic replacement does not alter significantly the thermodynamics of the system should be re-examined.

6. Acknowledgements

R.Y.-R. and I.S. thank the BSF – United States–Israel Binational Science Foundation. R.S.-C. would like to acknowledge the support of the Eshkol scholarship program of the Israel Ministry of Science and Technology. We thank Dr. Sofiya Kolusheva for her help with the HSDSC measurements.

7. References

- 1 I. Schmolka, *J. Am. Oil Chem. Soc.*, 1977, **54**, 110.
- 2 M. W. Edens, *Surf. Sci. Ser.*, 1996, **60**, 1.
- 3 I. R. Schmolka, *Cosmetics and Toiletries*, 1980, **95**, 77.
- 4 I. R. Schmolka, *Cosmetics and Toiletries*, 1984, **99**, 69.
- 5 T. Moon and R. Nagarajan, *Colloids Surf., A*, 1998, **132**, 275.
- 6 S.-Y. Lin and Y. Kawashima, *Pharm. Acta Helv.*, 1985, **60**, 339.
- 7 E. V. Batrakova, S. Li, V. U. Alakhov, D. W. Miller and A. V. Kabanov, *J. Pharmacol. Exp. Ther.*, 2003, **304**, 845.
- 8 S. D. Desai and J. Blanchard, *J. Pharm. Sci.*, 1998, **87**, 226.
- 9 K. Devanand and J. C. Sesler, *Nature*, 1990, **343**, 739.
- 10 G. Wanka, H. Hoffman and W. Ulbricht, *Macromolecules*, 1994, **27**, 4145.
- 11 P. Alexandridis and B. Lindman, *Amphiphilic Block Copolymers: Self-assembly and Applications*, Elsevier, Amsterdam/Lausanne/New York/Oxford, 2000.
- 12 A. Caragheorghopol and S. Schlick, *Macromolecules*, 1998, **31**, 7736–7745.
- 13 P. Alexandridis and T. A. Hatton, *Colloids Surf., A*, 1995, **96**, 1.
- 14 P. Alexandridis, U. O. Olsson and B. Lindman, *Langmuir*, 1998, **14**, 2627.
- 15 I. Goldmints, Ga-er Yu, C. Booth, K. A. Smith and T. A. Hatton, *Langmuir*, 1999, **15**, 1651.
- 16 S. Ruthstein, A. Potapov, A. M. Raitsimring and D. Goldfarb, *J. Phys. Chem. B*, 2005, **109**, 22843.
- 17 F. S. Bates, L. J. Fetters and G. D. Wignall, *Macromolecules*, 1988, **21**, 1086.
- 18 A. R. Esker, H. Gruell, G. Wegner, S. K. Satija and C. C. Han, *Langmuir*, 2001, **17**, 4688.
- 19 J. J. R. Stålgren, K. Boschkova, J.-C. Ericsson, C. W. Frank, W. Knoll, S. Satija and M. F. Toney, *Langmuir*, 2007, **23**, 11943.
- 20 A. Benschaul and I. Szleifer, *J. Chem. Phys.*, 1985, **83**, 3597.
- 21 I. Szleifer, *Curr. Opin. Colloid Interface Sci.*, 1996, **1**, 416–423.
- 22 C. B. E. Guerin and I. Szleifer, *Langmuir*, 1999, **15**, 7901–7911.
- 23 A. D. Mackie, A. Z. Panagiotopoulos and I. Szleifer, *Langmuir*, 1997, **13**, 5022.
- 24 I. Szleifer and M. A. Carignano, *Macromol. Rapid Commun.*, 2000, **21**, 423.
- 25 C. L. Ren, R. J. Nap and I. Szleifer, *J. Phys. Chem. B*, 2008, **112**, 16238.
- 26 I. Szleifer and M. A. Carignano, *Adv. Chem. Phys.*, 1996, **94**, 165.
- 27 J. Israelachvili, *Intermolecular and Surface Forces*. 2nd edn, London, Academic Press, 1992.
- 28 E. E. Dormidontova, *Macromolecules*, 2002, **35**, 987.
- 29 E. E. Dormidontova, *Macromolecules*, 2004, **37**, 7747.
- 30 J. Armstrong, B. Chowdhry, R. O'Brien, A. Beezer, J. Mitchell and S. Leharne, *J. Phys. Chem.*, 1995, **99**, 4590.
- 31 *Surfactant Solutions: New Methods of Investigation*, ed. R. Zana, Marcel Dekker, Inc., New York, Basel, 1987.
- 32 B. Z. Chowdhry, M. J. Snowden and S. A. Leharne, *Eur. Polym. J.*, 1999, **35**, 273–278.
- 33 I. Paterson, J. Armstrong, B. Chowdhry and S. Leharne, *Langmuir*, 1997, **13**, 2219.